Proceedings of the Institute of Acoustics

CROSS-CORRELATION FOR LEAK DETECTION IN BURIED PLASTIC WATER PIPES

Y Gao, M J Brennan, and P F Joseph
Institute of Sound and Vibration Research, University of Southampton, UK
Email: gy@isvr.soton.ac.uk

1 INTRODUCTION

Water leakage from buried pipes is a subject of increasing concern because of decreasing water supplies due to changing rainfall patterns, deterioration or damage to the distribution system, and ever increasing water demand. Leaks from water supply pipes generate noise, which can be used for leak detection and location. To achieve this the correlation technique is commonly used[1,2,3]. However, in general, satisfactory results have only been achieved with metal pipes. Plastic pipes have proved to be problematic, since the acoustic signals in these pipes are heavily attenuated and generally narrow-band and of low frequency.

Recent work by Hunaidi and Chu[4,5] on typical plastic water distribution pipes has focused on the dominant low frequency signals. They carried out an experimental investigation into the acoustic characteristics of several types of realistic leaks simulated under controlled conditions and found that most leak noise is concentrated at low frequencies. Although it has been shown that leaks in plastic pipes can be located using the correlation technique, the effectiveness of this technique has only been studied empirically.

Based on a theoretical formulation of wave propagation in a fluid-filled pipe *in vacuo* given in reference 6, and the assumption that the leak source spectrum is flat in the bandwidth of interest, this paper develops an analytical model to predict the cross-correlation function of leak signals in plastic pipes. The model explains some of the acoustic characteristics of the leak signal in buried plastic water pipes. Moreover, it is used to study the effects of the cut-off frequencies of high and low-pass digital filters used to remove noise, and the selection of acoustic/vibration sensors on the correlation technique. The theoretical work is validated with test data from actual water pipes.

2 LEAK DETECTION USING CORRELATION

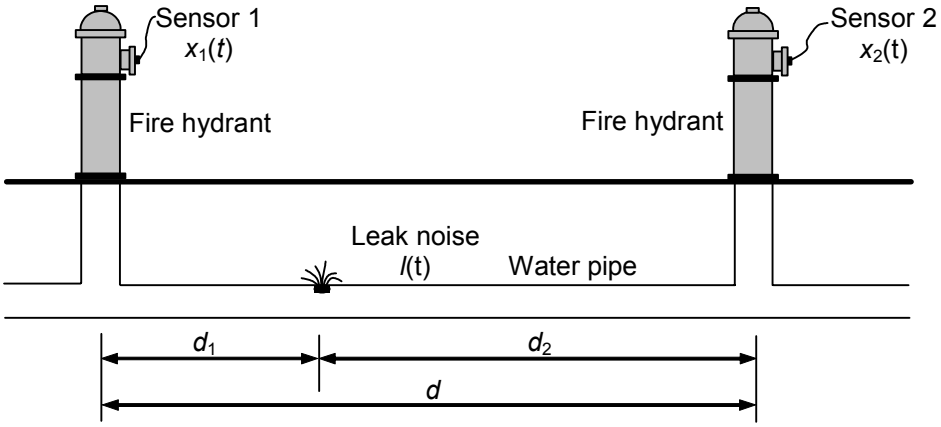

Figure 1. Schematic of a pipe with a leak bracketed by two sensors.

The cross-correlation technique for source location is straightforward. Vibration or acoustic signals are measured using either accelerometers or hydrophones at two access points, on either side of the location of a suspected leak. The signals from the sensors are input to the leak noise correlator, which computes the cross-correlation function of the two signals and presents the results to an operator. Figure 1 depicts a typical measurement arrangement for a leak in a buried water pipe. An access point (normally a fire hydrant) where a sensor can be attached is located on each side of the leak at distances d_1 and d_2. In the analysis presented in this paper the pipe is assumed to be of infinite length without reflecting discontinuities for the predominantly fluid-borne wave[6], at all frequencies of interest.

Consider the situation where the data measured are two continuous random signals $x_1(t)$ and $x_2(t)$, which are assumed to be stationary (ergodic). Setting the mean value of each signal to zero, the cross-correlation function is defined by[7]

$$R_{x_1x_2}(\tau) = E\left[x_1(t)x_2(t+\tau)\right], \tag{1}$$

where τ is the lag of time; and $E[\,]$ is the expectation operator. The argument τ that maximises equation (1) provides an estimate of the time delay τ_{peak}. It is useful to express the cross-correlation function in normalised form, which has a scale of –1 to +1, namely the correlation coefficient $\rho_{x_1x_2}(\tau)$ defined as

$$\rho_{x_1x_2}(\tau) = \frac{R_{x_1x_2}(\tau)}{\sqrt{R_{x_1x_1}(0)R_{x_2x_2}(0)}}, \tag{2}$$

where $R_{x_1x_1}(0)$ and $R_{x_2x_2}(0)$ are the values of auto-correlation functions at $\tau = 0$.

If a leak exists between the two sensor positions, a distinct peak may be found in the cross-correlation function. This gives the time delay τ_{peak} that corresponds to the difference in arrival times between the signals at each sensor. The location of the leak relative to one of the measurement points is easily calculated using the simple algebraic relationship between the time delay τ_{peak}, the distance d between the access points, and the propagation wavespeed c in the buried pipe,

$$d_1 = \frac{d - c\tau_{peak}}{2}. \tag{3}$$

3 COMBINING THE CORRELATION TECHNIQUE WITH THE WAVE PROPAGATION MODEL

3.1 Cross-correlation using pressure, velocity and acceleration responses

Leak noise in water-filled plastic pipes is concentrated at low frequencies. In this frequency range the predominantly fluid-borne axisymmetric wave carries most of the acoustic energy generated by the leak[6,8]. In this section, models of the cross-correlation functions for pressure, velocity and acceleration responses are derived and discussed.

The frequency response function between the pressure measured at the sensor location and at the leak location, $H^p(\omega, x)$, is given by[9]

$$H^p(\omega, x) = e^{-i\omega x/c}e^{-\omega\beta x}, \tag{4}$$

where x is the distance between the leak and sensor signals; and β is a measure of the loss within the pipe wall. Previous work shows that there is a linear relationship between the pipe wall displacement and the internal pressure[10]. The frequency response functions of the pressure, velocity and acceleration measured at the sensor location and the pressure at the leak location are thus given by

$$H(\omega, x) = (i\omega)^n A_n e^{-i\omega x/c} e^{-\omega\beta x} . \quad (5)$$

When n=0, 1 and 2, equation (5) gives the frequency response functions of pressure, velocity and acceleration respectively. Here $A_0 = 1$, $A_1 = A_2 = \frac{a^2}{Eh}$; E is the Young's modulus of the pipe wall; a and h are the mean pipe radius and pipe wall thickness respectively.

Figure 2 shows the frequency response functions given by equation (5), where all the frequency response functions are normalised to their respective maximum amplitudes. The frequency response function of pressure, $H^p(\omega, x)$, decreases exponentially with increasing frequency, so acts as a low pass filter whereby higher frequencies are attenuated at a faster rate than low frequencies. In contrast, both the frequency response functions of velocity, $H^v(\omega, x)$, and acceleration, $H^a(\omega, x)$, behave as band-pass filters, with the latter having a higher "centre" frequency and a broader bandwidth, thus allowing more high frequency information to pass.

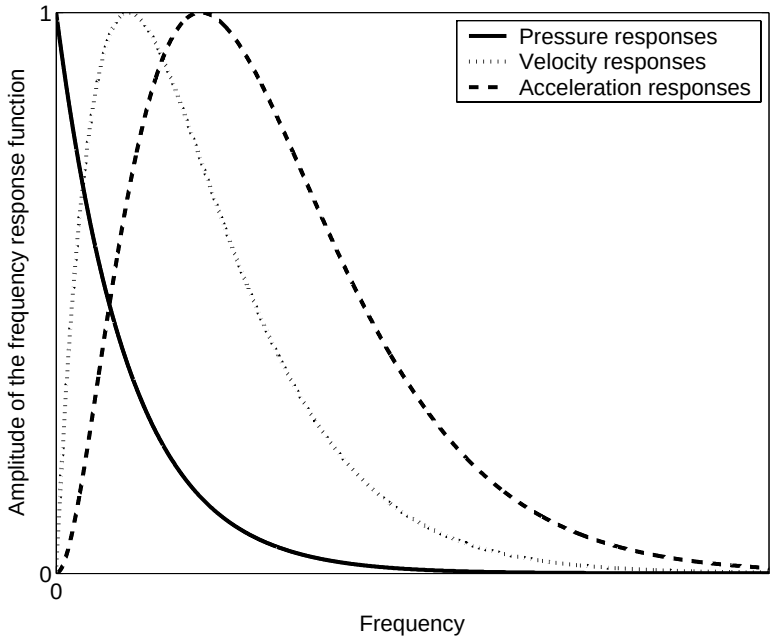

Figure 2. Illustration of the amplitude of the frequency response function.
All the frequency responses are normalised to the corresponding maximum amplitudes.

Referring to Figure 1, the cross-spectral density $S_{x_1x_2}(\omega)$ for two signals $x_1(t)$ and $x_2(t)$ measured at positions $x = d_1$ and $x = d_2$, is given by

$$S_{x_1x_2}(\omega) = \frac{1}{2\pi} \lim_{T\to\infty} E\left[\frac{X_{1T}^*(\omega) X_{2T}(\omega)}{T}\right] = S_{II}(\omega) H^*(\omega, d_1) H(\omega, d_2) , \quad (6)$$

where $S_{ll}(\omega)$ is the auto-spectral density of the leak signal $l(t)$, which is the acoustic pressure at the leak location. Combining equations (5) with (6) gives the cross-spectral density as

$$S_{x_1x_2}(\omega) = A_n^2 S_{ll}(\omega)\Psi_{2n}(\omega)e^{i\omega T_0}\,, \tag{7}$$

where $\Psi_{2n}(\omega) = \omega^{2n}\Psi(\omega)$; $\Psi(\omega) = \left|H^{p^*}(\omega,d_1)H^{p}(\omega,d_2)\right| = e^{-\omega\beta d}$; $T_0 = -(d_2 - d_1)/c$ is the time delay. When n=0, 1 and 2, equation (7) gives the cross-spectral density for pressure, velocity and acceleration signals respectively. The corresponding phase spectrum that is related to the time shift experienced by the signals as they propagate along the pipe, is given by

$$\Phi_{x_1x_2}(\omega) = Arg\left\{S_{x_1x_2}(\omega)\right\} = \omega T_0\,. \tag{8}$$

It is clear from equation (8) that the phase spectrum is independent of the choice of acoustic/vibration sensors. Since multiplication in one domain corresponds to convolution in the transformed domain, the cross-correlation function $R_{x_1x_2}(\tau)$ is determined by

$$R_{x_1x_2}(\tau) = F^{-1}\left\{S_{x_1x_2}(\omega)\right\} = A_n^2 R_{ll}(\tau)\otimes\psi_{2n}(\tau)\otimes\delta(\tau+T_0)\,, \tag{9}$$

where $F^{-1}\{\ \}$ denotes the inverse Fourier transform; $\otimes$ denotes convolution; $R_{ll}(\tau) = F^{-1}\left\{S_{ll}(\omega)\right\}$ is the auto-correlation of the leak signal; $\psi_{2n}(\tau) = F^{-1}\left\{\Psi_{2n}(\omega)\right\}$; and $\delta(\tau)$ is the Dirac delta function. An interpretation of equation (9) is that the delta function $\delta(\tau+T_0)$ is broadened by the introduction of the leak spectrum $S_{ll}(\omega)$ and the frequency behaviour of $\Psi_{2n}(\omega)$. Thus, even if $S_{ll}(\omega)$ is a constant S_0, the delta function is smeared because of the frequency attenuation of the leak signal. Reliable leak detection can only be accomplished when a peak can be distinguished in the cross-correlation function. A sharp peak rather than a smeared broad one is required to achieve accurate estimation of the time delay. Because the behaviour of $\Psi_{2n}(\omega)$ is governed by the choice of acoustic/vibration sensors, selection of appropriate sensors may offer improvement of the time delay estimation from the cross-correlation of the leak noise. This is addressed below.

3.2 Selection of acoustic/vibration sensors

Using the relationship $\psi_{2n}(\tau) = (-1)^n \dfrac{d^{2n}\psi(\tau)}{d\tau^{2n}}$, equation (9) can be reformulated as

$$R_{x_1x_2}(\tau) = (-1)^n A_n^2 R_{ll}(\tau)\otimes\frac{d^{2n}\psi(\tau)}{d\tau^{2n}}\otimes\delta(\tau+T_0)\,, \tag{10}$$

where $\psi(\tau) = F^{-1}\left\{\Psi(\omega)\right\} = \dfrac{\beta d}{\pi\left[(\beta d)^2+\tau^2\right]}$. Assuming $S_{ll}(\omega) = S_0$, equation (10) becomes

$$R_{x_1x_2}(\tau) = (-1)^n A_n^2 S_0 \frac{d^{2n}\psi(\tau+T_0)}{d\tau^{2n}}\,. \tag{11}$$

Following a similar analysis to that for the cross-correlation function of two sensor signals, the auto-correlation function is given by

$$R_{xx}(\tau) = (-1)^n A_n^2 S_0 \frac{d^{2n}\varphi(\tau)}{d\tau^{2n}}. \tag{12}$$

Combining equations (11), (12) with (2) gives the cross-correlation coefficient as

$$\rho_{x_1x_2}(\tau) = \frac{\dfrac{d^{2n}\psi(\tau+T_0)}{d\tau^{2n}}}{\sqrt{\left.\dfrac{d^{2n}\varphi(0)}{d\tau^{2n}}\right|_{x=d_1} \left.\dfrac{d^{2n}\varphi(0)}{d\tau^{2n}}\right|_{x=d_2}}}. \tag{13}$$

The corresponding correlation coefficients for pressure, velocity and acceleration signals, are discussed below:

1) For pressure signals, (n=0), equation (13) becomes

$$\rho_{x_1x_2}(\tau) = \frac{2\sqrt{d_1d_2}}{d} \frac{(\beta d)^2}{(\beta d)^2 + (\tau + T_0)^2}. \tag{14a}$$

2) For velocity signals, (n=1), equation (13) becomes

$$\rho_{x_1x_2}(\tau) = \left(\frac{2\sqrt{d_1d_2}}{d}\right)^3 \left[\frac{(\beta d)^2}{(\beta d)^2 + (\tau + T_0)^2}\right]^2 \left\{1 - \frac{4(\tau + T_0)^2}{(\beta d)^2 + (\tau + T_0)^2}\right\}. \tag{14b}$$

3) For acceleration signals, (n=2), equation (13) becomes

$$\rho_{x_1x_2}(\tau) = \left(\frac{2\sqrt{d_1d_2}}{d}\right)^5 \left[\frac{(\beta d)^2}{(\beta d)^2 + (\tau + T_0)^2}\right]^3 \left\{1 - \frac{12(\tau + T_0)^2}{(\beta d)^2 + (\tau + T_0)^2} + \frac{16(\tau + T_0)^4}{\left[(\beta d)^2 + (\tau + T_0)^2\right]^2}\right\}. \tag{14c}$$

To clarify further the effect of the selection of acoustic/vibration sensors on the correlation technique, the peak cross-correlation coefficient is investigated. When $\tau = -T_0$, equations (14a,b,c) give

$$\rho_{x_1x_2}(\tau_{peak}) = \left(\frac{2\sqrt{d_1d_2}}{d}\right)^{2n+1} = \left(\frac{2\sqrt{d_1/d_2}}{1 + d_1/d_2}\right)^{2n+1}. \tag{15}$$

Equations (14a,b,c) show that the correlation coefficients are dominated by both the loss of the pipe, β, and the locations of two sensors, d_1 and d_2. Interestingly, the peak values of the correlation coefficients given by equation (15) are only related to the ratio of the relative distances d_1/d_2, and not on their absolute values. Figure 3 shows the peak values of the cross-correlation coefficients given by equation (15) as a function of d_1/d_2. It can be seen that for two equispaced sensors, the peak cross-correlation coefficients are all unity. Altering the ratio d_1/d_2, the peak value of the pressure responses changes slowly by comparison with those given by the velocity and acceleration responses. This shows that for leak detection measurements, where $d_1 \neq d_2$, which is the most likely situation in practice, the pressure signals give the largest cross-correlation coefficient. Moreover, good levels of correlation (e.g., greater than about 0.5) are only possible when the ratio of distances satisfies $1/10 \le d_1/d_2 \le 10$, $1/4 \le d_1/d_2 \le 4$ and $1/3 \le d_1/d_2 \le 3$ for pressure, velocity and acceleration responses respectively. Otherwise, the peak correlation values of the velocity and acceleration responses rapidly become very small. Therefore, for low levels of leak signals, namely in a small signal to noise ratio (SNR) environment, a measure of pressure responses is necessary, since in this case the correlation coefficient gives a large peak value, which is less sensitive to the

relative distance of the sensor locations. In practical situations, the achievement of cross-correlation coefficients with clear (or definite) peaks will be further constrained because of band-pass filtering and background noise.

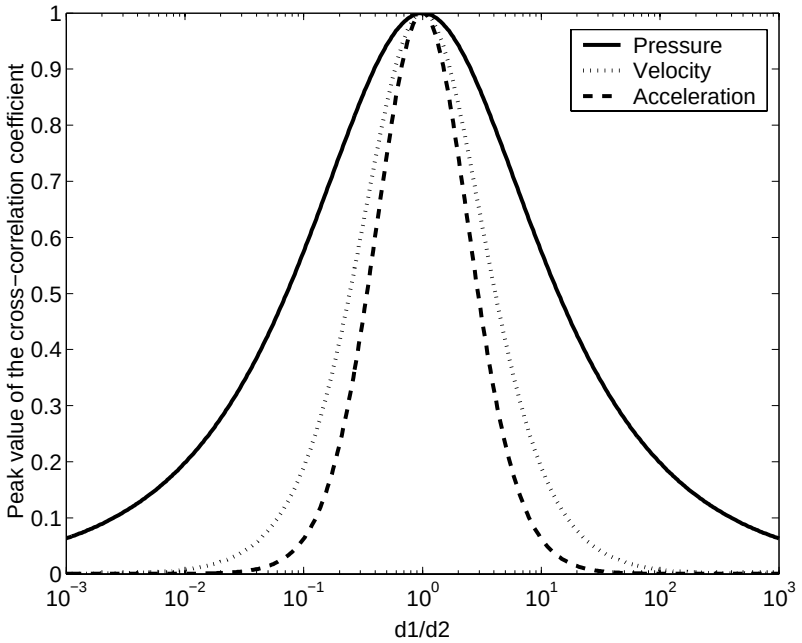

Figure 3. Peak value of the cross-correlation coefficient as a function of d_1/d_2.

The behaviour of the peak value of the cross-correlation coefficient exhibited in Figure 3 is easily explained in physical terms. When leak sensors are equidistant from the leak source, leak signals will be identical and therefore will lead to the largest peak cross-correlation coefficient. As the ratio between leak sensor distances, d_1/d_2, becomes larger or smaller, the similarity between the sensor signals diminishes due to the frequency dependence of attenuation rates. Pressure responses give the highest peak cross-correlation coefficient because they have the least high frequency content and hence are least affected by attenuation. In practical situations, background noise also has an effect on the correlation. In section 4 the theoretical predictions are compared with experimental data, which, inevitably, will be contaminated by noise. To make this comparison, therefore, the effect of noise on the peak correlation needs to be included in the model, which has been discussed in reference 9.

To accurately determine the position of a leak, a sharp (narrow) peak in the cross-correlation function is desirable. The way in which the cross-correlation obtained from pressure, velocity, and acceleration responses affects the peak is now investigated. We define a cross-correlation width, $\Delta\tau$, as the time between the first two zero crossings given by $\rho_{x_1x_2}(\tau_{peak} \pm \Delta\tau/2) = 0$. The behaviour of $\Delta\tau$ for the various correlation functions is as follows,

1) For pressure responses, equation (14a) shows that the width $\Delta\tau$ is undefined as the cross-correlation has no zero crossings, and hence $\Delta\tau = \infty$. However, the 3dB width of the peak in the cross-correlation function is found to be[10]

$$\Delta\tau \approx 2\beta d \,. \tag{16a}$$

2) For velocity responses, from equation (14b), the width, $\Delta\tau$ is determined to be

$$\Delta\tau = \frac{2}{\sqrt{3}}\beta d\ . \tag{16b}$$

3) For acceleration responses, from equation (14c), $\Delta\tau$ is determined to be

$$\Delta\tau = \frac{2}{\sqrt{5+2\sqrt{5}}}\beta d\ . \tag{16c}$$

For different sensor signals, it can be seen that the width of the peak in the cross-correlation function is proportional to the product βd. Thus, for leak detection in pipes with small attenuation (small β), as in the case of metal pipes, a sharp peak can be easily achieved using the correlation technique. In contrast, for plastic pipes with large attenuation (large β), a relatively short distance between two sensor locations is often required for the estimation of time delay from the cross-correlation function. By comparing the cross-correlation width given by equations (16a,b,c), it can be seen that the correlation between acceleration signals provides the sharpest peak in the correlation function, while the broadest peak occurs for pressure signals. It is found, therefore, that a sharp peak can be achieved by using the acceleration responses at the expense of a low peak value of the correlation coefficient.

3.3 The effect of band-pass filtering on the correlation technique

For most plastic pipework systems, leak detection is successful with low frequency leak signals resulting from a non-dispersive propagating wave with a constant attenuation factor β. In practice, band-pass filtering operations are performed to attenuate the signals outside the frequency range of interest. If the signals are band-passed filtered using an ideal filter, $G(\omega)$, which is equal to unity if $\omega_0 \le |\omega| < \omega_1$ and zero otherwise, the cross-correlation function given by equation (11) becomes

$$R_{x_1x_2}(\tau) = (-1)^n A_n^2 S_0 \frac{d^{2n}\psi(\tau)}{d\tau^{2n}} \otimes g(\tau + T_0)\ , \tag{17}$$

where $g(\tau) = F^{-1}\{G(\omega)\} = \frac{\Delta\omega}{\pi}\frac{\sin(\Delta\omega\tau/2)\cos(\omega_c\tau)}{\Delta\omega\tau/2}$; the frequency band $\Delta\omega = \omega_1 - \omega_0$ and the central frequency $\omega_c = (\omega_0 + \omega_1)/2$. It can be seen that the effect of band-pass filtering is to introduce a ripple with frequency ω_c into the cross-correlation modulated by the bandwidth $\Delta\omega$. Equation (17) also shows that the delta function is further smeared by the introduction of band-pass filtering. Specifically, for pressure signals, the effect of band-pass filtering is discussed in this paper. In this case, the cross-correlation function given by equation (17) changes to be

$$R_{x_1x_2}(\tau) = \frac{S_0 e^{-\omega_0\beta d}}{\pi\sqrt{(\beta d)^2 + (\tau + T_0)^2}}\left\{\cos[\omega_0(\tau + T_0) + \theta] - e^{-\Delta\omega\beta d}\cos[\omega_1(\tau + T_0) + \theta]\right\}, \tag{18}$$

where $\theta = \tan^{-1}[\tau/(\beta d)]$. If the frequency bandwidth satisfies the condition $e^{-\Delta\omega\beta d} \ll 1$, equation (18) can be approximated by

$$R_{x_1x_2}(\tau) \approx \frac{S_0 e^{-\omega_0\beta d}}{\pi\sqrt{(\beta d)^2 + (\tau + T_0)^2}}\cos[\omega_0(\tau + T_0) + \theta]\ . \tag{19}$$

Compared with equation (18), the interference term caused by the upper cut-off frequency ω_1 does not appear in equation (19). Thus it can be seen that, provided that the bandwidth of the filter is relatively broad, the cross-correlation function is mainly dominated by the lower cut-off frequency

ω_0. This is because the pipe effectively acts as a low-pass filter, due to damping in the pipe-wall as shown in equation (4).

4 EXPERIMENTAL WORK

Tests were carried out at a leak detection facility at an experimental site located at a National Research Council site in Canada. The description of the test site and measurement procedures are detailed in reference 4. Signals from a joint leak were measured using hydrophones and accelerometers. The hydrophones and accelerometers were both attached to two fully pressurised fire hydrants. Referring to Figure 1, the distance *d* between the two sensor signals was 102.6m, and the distance d_1 from the leak to sensor 1 was 73.5m. The signals were each passed through an anti-aliasing filter with the cut-off frequency set at 200Hz. Hydrophone-measured signals of 66-second duration were then digitised at a sampling frequency of 500samples/second. The same sampling frequency was applied to the accelerometer-measured signals for the time duration of 60 seconds.

Spectral analysis was performed on the digitised data using a 1024-point FFT, and a Hanning window and power spectrum averaging were applied. The propagation wavespeed can be determined from the cross-spectral density between two sensor signals. The phase spectra obtained from the hydrophone and accelerometer-measured signals are shown in Figures 4(a) and (b). As discussed in reference 10, based on the slope of the unwrapped phase angle plotted in Figures 4(a) and (b), the wavespeed calculated is 479m/s and 484m/s for hydrophone and accelerometer-measured signals respectively. The attenuation factor β is 2.26×10^{-4}s/m [9].

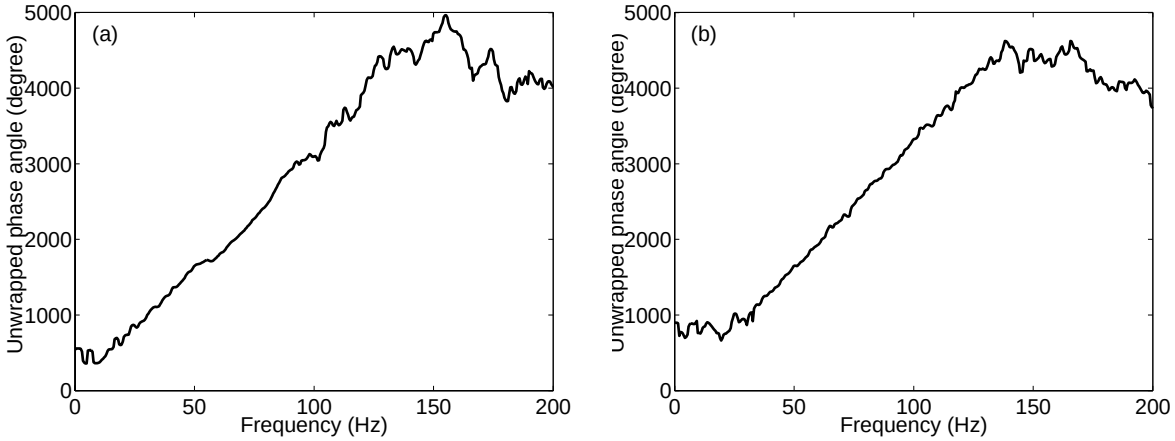

Figure 4. Unwrapped phase angle for
(a) Hydrophone-measured signals; (b) Accelerometer-measured signals.

Noting that the measured signals were dominated by the ambient noise at low frequencies and attenuated at high frequencies[10], filtering operations were performed on the digitised sensor signals before conducting the time domain cross-correlation. The sensor signals were then passed through high and low-pass 4th order Butterworth filters. The cross-correlation coefficients were computed using segment averaging via a 1024-point FFT and the circular effect of the FFT was reduced by 50% zero padding in each segment record. To compare the experimental results with the corresponding theoretical predictions, the effect of the background noise on the theoretical predictions was taken into account by setting the peak values of the cross-correlation coefficients to be the same as those of the experimental results.

4.1 Analysis of hydrophone-measured signals

The effect of the low-pass filter cut-off frequency on the cross-correlation coefficient is demonstrated in Figure 5. The filter cut-off frequencies were set at 10Hz for the high-pass filter, and the cut-off frequencies ranged from 30Hz to 200Hz for the low-pass filters. In the theoretical model, the cross-correlation coefficient is mainly determined by the lower cut-off frequency, provided that the bandwidth of the leak noise is relatively broad. This effect can be seen by comparing Figures 5(d), (f) with (h), which are very similar. In contrast, a slight difference can be seen in Figure 5(b) because in this case the theoretical correlation coefficient is governed by both the lower and upper cut-off frequencies as the bandwidth is small. A similar trend can be seen in the experimental results plotted in Figures 5(a) and (c), where there is a slight difference in the correlation coefficients when the low-pass filters are set at 30Hz and 50Hz. Furthermore, when the low-pass filter cut-off frequencies are adjusted to values above 50Hz, the correlation coefficients do not change as shown in Figures 5(e) and (g). This indicates that most information about the leak signal is concentrated below 50Hz and the ambient noise measured by the hydrophones dominates above 50Hz. Thus for hydrophone-measured signals in this case, the low-pass filter cut-off frequency can be set at 50Hz.

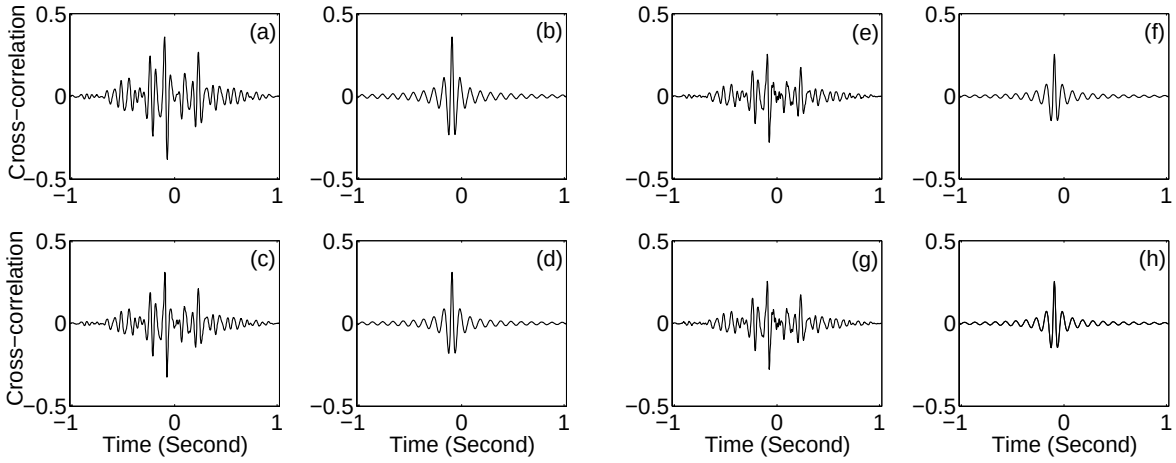

Figure 5. Effect of the low-pass filter cut-off frequency on the cross-correlation coefficient. The cut-off frequencies of the high-pass filters are set at 10Hz. The low-pass filter cut-off frequencies are: (a) 30Hz; (c) 50Hz; (e) 100Hz; (g) 200Hz. Comparison of the corresponding theoretical values is made when the low-pass filter cut-off frequencies are set at: (b) 30Hz; (d) 50Hz; (f) 100Hz; (h) 200Hz.

Figure 6 shows the effect of the high-pass filter cut-off frequency for both experimental results and predictions. The cut-off frequencies of the low-pass filters are 50Hz and those of the high-pass filters from 5Hz to 40Hz. For the correlation coefficients derived from the hydrophone-measured signals as shown in Figures 6(c), (e) and (g), a definite peak is obtained despite the narrow frequency band of the leak signal. The oscillatory behaviour of the correlation function becomes more obvious as the pass band of the leak signal becomes smaller. The time delay is estimated to be in the range 0.090s to 0.094s and the position of the leak relative to point 1 is calculated to be 72.9m to 73.8m. However, three anomalous peaks can be seen in Figure 6(a), which are caused by the interference of low frequency background noise at low frequencies below 10Hz and may present false time delay estimators. In addition, a definite peak cannot always be obtained when the cut-off frequency of the high-pass filter is set below 10Hz, as expected. Thus the high-pass filter cut-off frequency can be set at 10Hz. The corresponding theoretical values of the cross-correlation coefficients are plotted in Figures 6(b), (d), (f) and (h). These graphs illustrate the same oscillatory behaviour of the correlation coefficients to that of the experimental results. The differences between the predictions and the experimental results are due to the effect of the background noise on the measured signals.

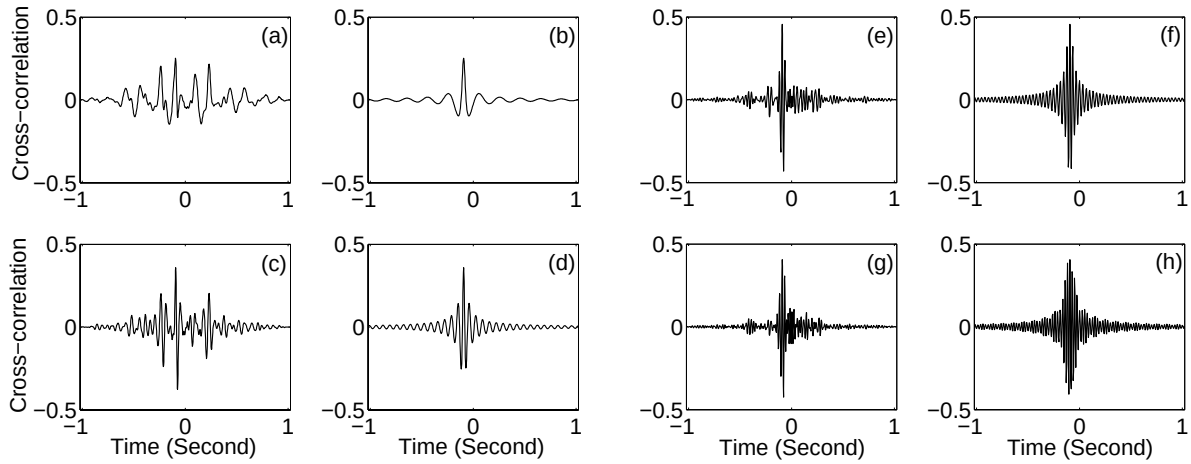

Figure 6. Effect of the high-pass filter cut-off frequency on the cross-correlation coefficient. The cut-off frequencies of the low-pass filters are set at 50Hz. The high-pass filter cut-off frequencies are: (a) 5Hz; (c) 15Hz; (e) 30Hz; (g) 40Hz. Comparison of the corresponding theoretical values is made when the high-pass filter cut-off frequencies are set at: (b) 5Hz; (d) 15Hz; (f) 30Hz; (h) 40Hz.

4.2 Comparison of the cross-correlation using different sensors

The cut-off frequencies of the digital filters can be chosen using the phase spectrum between two sensor signals plotted in Figures 4(a) and (b). The lower and upper cut-off frequencies were set at 10Hz and 50Hz for hydrophone-measured signals as discussed in section 4.1, and 30Hz and 140Hz for accelerometer-measured signals. It has been shown in reference 9 that an estimate of the SNR at a measurement position can be simply determined from the ratio of the peak values of the experimental result of the correlation coefficient and its corresponding theoretical prediction in the noise-free case. The SNR was found to be –6.7dB and 2.7dB at positions where hydrophones 1 and 2 were attached and -10.9dB and 14.6dB at positions where accelerometers 1 and 2 were attached respectively.

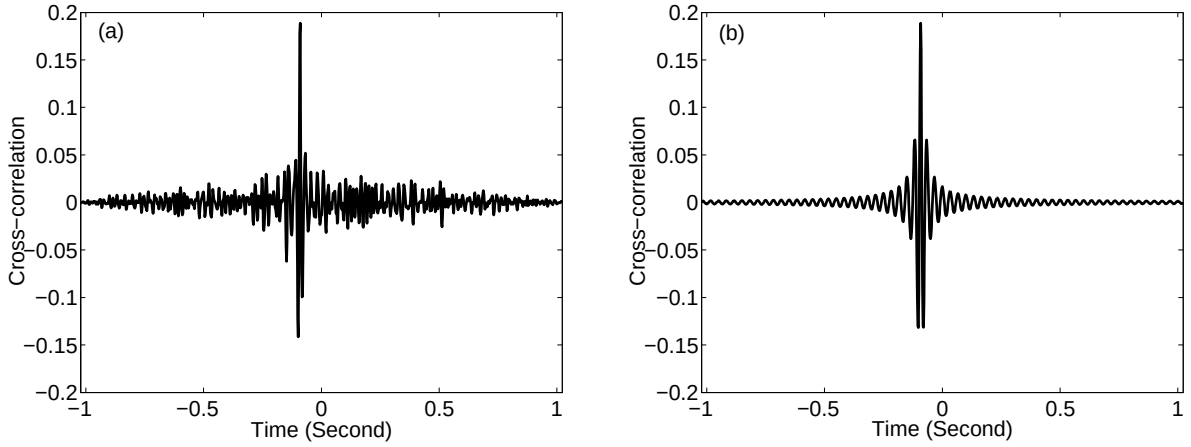

Figure 7. Cross-correlation using accelerometer-measured signals:
(a) Cross-correlation; (b) Theoretical prediction. The pass band of the ideal filter is 30-140Hz.

The cross-correlation coefficients using accelerometer-measured signals and the corresponding theoretical prediction are plotted in Figure 7. Compared with the hydrophone-measured signals plotted in Figure 5(c), Figure 7(a) shows that the correlation coefficient obtained from accelerometer-

measured signals produces a more pronounced but lower peak value. The distance d_1 is found to be 73.1m, which is determined from the time delay of 0.090s. The corresponding theoretical prediction plotted in Figure 7(b) illustrates very similar high frequency behaviour of the correlation coefficient.

5 CONCLUSIONS

An analytical model of the cross-correlation function for wave propagation in buried plastic water pipes has been established in this paper. The modal is used to evaluate the effectiveness of the correlation technique for leak detection in plastic water distribution pipes. Theoretical predictions of the correlation functions show the following:

- The use of pressure signals leads to the highest peak cross-correlation coefficient. Therefore, a measure of pressure responses using hydrophones would be the most suitable for locating leaks having small SNR. This is consistent with practical experience.

- Pressure signals are the least sensitive to the relative positions of the sensors and therefore are the most suitable for extreme positions. Good levels of peak cross-correlation coefficient (e.g., greater than about 0.5) are only possible when the ratio of distances satisfies $1/10 \le d_1/d_2 \le 10$, $1/4 \le d_1/d_2 \le 4$ and $1/3 \le d_1/d_2 \le 3$ for pressure, velocity and acceleration responses respectively. In practice, these limits will be less stringent due to the limited bandwidth of the leak source and background noise.

- The use of acceleration signals results in the sharpest peak of the cross-correlation coefficient. It also exhibits the least spreading of the envelope. This suggests that accelerometers are most suitable in multi-leak and coherent noise situations.

- For pressure signals, the model explains the importance of the cut-off frequency of the high-pass filter and the insensitivity of the correlation to the cut-off frequency of the low-pass filter to measurements of the cross-correlation.

The theoretical predictions have been validated by comparison with results obtained using real leak signals measured by hydrophones and accelerometers.

6 REFERENCES

1. Fantozzi, M., G.D. Chirico, E. Fontana, and F. Tonolini, Leak inspection on water pipelines by acoustic emission with cross-correlation method, in Annual Conference Proceeding, American Water Works Association, Engineering and Operations, San Antonio (1993).
2. Fuchs, H.V. and R. Riehle, Ten years of experience with leak detection by acoustic signal analysis, Applied Acoustics. 33(1) 1-19. (1991).
3. Liston, D.A. and J.D. Liston, Leak detection techniques, Journal of the New England Water Works Association. 106(2) 103-108. (1992).
4. Hunaidi, O., W. Chu, A. Wang, and W. Guan, Detecting leaks in plastic pipes, Journal American Water Works Association. 92(2) 82-94. (2000).
5. Hunaidi, O. and W.T. Chu, Acoustical characteristics of leak signals in plastic water distribution pipes, Applied Acoustics. 58(3) 235-254. (1999).
6. Pinnington, R.J. and A.R. Briscoe, Externally applied sensor for axisymmetric waves in a fluid filled pipe, Journal of Sound and Vibration. 173(4) 503-516. (1994).
7. Oppenheim, A.V. and R.W. Schafer, Digital Signal Processing, Englewood Cliffs, NJ: Prentice-Hall. (1975).

8. Muggleton, J.M., M.J. Brennan, and R.J. Pinnington, Wavenumber prediction of waves in buried pipes for water leak detection, Journal of Sound and Vibration. 249(5) 934-954. (2002).
9. Gao, Y., M.J. Brennan, P.F. Joseph, J.M. Muggleton, and O. Hunaidi, A model of the correlation function of leak noise in buried plastic pipes, Journal of Sound and Vibration. (2003 Accepted to publish).
10. Gao, Y., M.J. Brennan, P.F. Joseph, and J.M. Muggleton, Use of cross-correlation for leak detection in plastic pipes, ISVR Technical Memorandum No. 901. (2002).